Additive Manufacturing: Metallurgy, Cut Analysis & Porosity

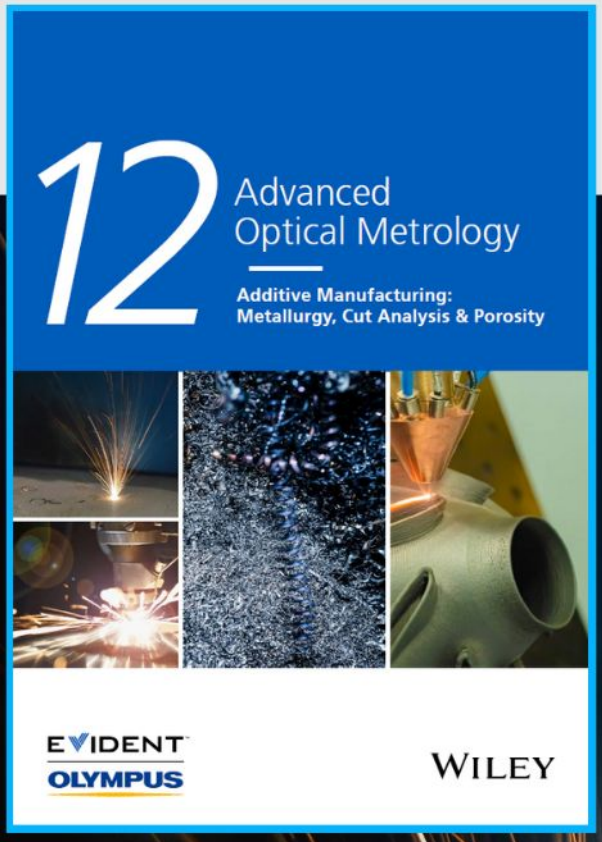

The latest eBook from Advanced Optical Metrology. Download for free.

In industry, sector after sector is moving away from conventional production methods to additive manufacturing, a technology that has been recommended for substantial research investment.

Download the latest eBook to read about the applications, trends, opportunities, and challenges around this process, and how it has been adapted to different industrial sectors.

EVIDENT
OLYMPUS

WILEY

NANO · MICRO small
www.small-journal.com

A Mutual Boosting Self-Excitation Hybrid Cell for Harvesting High Entropy Energy at 32% Efficiency

Jun Wu, Wenlin Liu, Qixuan Zeng, Ying Zhang, Hengyu Guo, Xiaofang Zhang, Wencong He, Yanlin Luo, Xue Wang, and Zhong Lin Wang**

Triboelectric nanogenerators (TENGs) and dielectric elastomer generators (DEGs) are potentially promising energy conversion technologies, but they still have limitations due to their own intrinsic characteristics, including the low energy output of TENGs caused by the air breakdown effect, and external polarization voltage requirement for DEGs, which severely limit their practical applications. Herein, coupling TENG with DEG is proposed to build a mutual beneficial self-excitation hybrid generator (named TDHG) for harvesting distributed and low-quality mechanical energy (high entropy energy). Experimental results demonstrate that the output charges of this TDHG are enhanced by fivefold of that of the conventional charge-excitation TENG, and continuous operation of DEG is also realized by simple mechanical triggering. More importantly, owing to the high peak power contributed by TENG and the long output pulse duration guaranteed by DEG, the TDHG realizes a much higher energy conversion efficiency of 32% in comparison to either the TENG (3.6%) or DEG (13.2%). This work proposes a new design concept for hybridized energy harvester toward highly efficient mechanical energy harvesting.

1. Introduction

In the era of the Internet of Things (IoT),[1,2] ubiquitous sensor network nodes bring convenience to both daily life and industrial production, while facing huge energy supply challenges.[3–5] To meet the rapidly increased energy demands, a newly emerging energy harvesting technology, triboelectric nanogenerators (TENGs), has been invented to convert ambient mechanical energy into electric power based on the coupling effects of triboelectrification and electrostatic induction.[6] Such energy is widely distributed, low-amplitude and low-frequency, and is referred as high entropy energy. Due to its advantages of high-efficiency, low cost, and easy fabrication,[7–9] TENGs has achieved great applications in energy harvesting,[10–14] self-powered sensors,[15–20] and direct high-voltage power sources.[21–23] Currently, the key challenge for TENGs should be the relatively low energy output capability.[2,24,25] To compensate for this shortcoming, a promising direction is to integrate TENG with other transducing prototypes, for example, electromagnetic generator,[26,27] piezoelectric nanogenerator,[28] and thermoelectric generator.[29] Although better performances could be achieved by these hybrid devices, generators are quite different in structures and principles, leading to distinct output characteristics of the components. Furthermore, it has been recognized that the output energy of TENG should be directly determined by its charge density.[2,24] Therefore, the way to improve the charge density of TENGs has become a focused research area, including material modification,[30,31] ion injection,[32] and external-charge pumping.[33,34] Nevertheless, the improving rate is still limited (hundreds of $\mu C\ m^{-2}$). Very recently, a charge excitation TENG system was proposed.[35] Relying on the auto-switch of capacitors in external circuit between series and parallel, an exponential charge accumulation was realized, producing a milestone charge density of 1.25 $mC\ m^{-2}$. This work suggests that employing an excitation circuit could be a promising strategy for achieving high-output TENGs. However, the air gap between two triboelectric surfaces will lead to air breakdown under high voltage, and thereby causes a sharp decline of transferred charge quantity. Although the output performance can be further enhanced by controlling the atmospheric environment,[36,37] the restriction of air breakdown effect is not overcome in essence. Therefore, developing strategies for minimizing the limitation of air breakdown is highly desired for pushing the power generation of charge-excitation TENG to a new horizon.

Similar to TENG, dielectric elastomer generator (DEG) is a class of electrostatic soft transducer capable of converting

J. Wu, W. Liu, Q. Zeng, Y. Zhang, H. Guo, X. Zhang, W. He, Y. Luo, X. Wang
Department of Applied Physics
State Key Laboratory of Power Transmission Equipment & System Security and New Technology
Chongqing University
Chongqing 400044, P. R. China
E-mail: xuewang@cqu.edu.cn

Z. L. Wang
Beijing Institute of Nanoenergy and Nanosystems
Chinese Academy of Sciences
Beijing 100083, P. R. China
E-mail: zhong.wang@mse.gatech.edu

Z. L. Wang
School of Material Science and Engineering
Georgia Institute of Technology
Atlanta, GA 30332-0245, USA

The ORCID identification number(s) for the author(s) of this article can be found under https://doi.org/10.1002/smll.202205704.

DOI: 10.1002/smll.202205704

mechanical energy into electric power based on the capacitance difference between stretched and released states.[38–40] Over the past decades, DEG is considered as a very promising energy conversion technology due to its attributes of lightweight, low cost, good coupling with many mechanical inputs, and flexible design.[38–41] More importantly, there is no air-gap between electrode and dielectric film in DEG, that is to say, under a high-voltage situation, only dielectric breakdown can occur, which is much more difficult than air breakdown,[42,43] ensuring a superior energy output per unit mass (up to 0.78 J g^{-1}).[44] Nevertheless, to date, DEGs are not well applied in practical aspect due to the requirement of an external bias voltage source to perform the energetic cycles.[41,45,46] To address this problem, different solutions for autonomous DEG have been proposed. Mc Kay et al. presented an integrated self-priming circuit, in which a portion of the generated energy of a first DEG was used as extra charges for the energetic cycle of the second DEG.[47] Although periodic external charge injections had been eliminated, it still required an initial amount of charges to get started. Besides, some hybrid systems were also investigated, such as coupling DEGs with piezoelectric generators[48] or electret generators.[49] These strategies can overcome the shortages of DEGs in some sense, but still face drawbacks such as distinct working principles and mechanical properties of excitation generators.

Considering both of TENG and DEG can be equivalent to variable-capacitor generators, which hold similar energy conversion mechanisms as well as comparable mechanical properties, herein, we present fabrication of a hybrid generator that is composed of TENG and DEG (named as TDHG) for the first time. By connecting TENG and DEG in parallel into a self-excitation circuit (SEC), mechanical energy can be effectively converted into electric power through synergistic using of these two transducers. Benefitting from this novel design, the voltage generated by TENG can act as polarization source for DEG, while the no air-gap configuration of DEG can guarantee an exceptional energy output. The working mechanism and output performance of the as-fabricated TDHG are systematically studied. After optimization, the charge of TENG, DEG, and TDHG can reach up to 1.03, 3.03, and 5.05 μC, respectively. That is to say, after assembling, the amount of output charges of the TDHG is enhanced by fivefold in comparison to that of the normal charge-excitation TENG generated, and continuous operation of DEG is also achieved by simple mechanical triggering. More importantly, owing to the mutual beneficial interaction between the two components, the TDHG realizes a much higher energy conversion efficiency (32%) either compared to sole TENG (3.6%) or DEG (13.2%), further confirming the superiority of this novel hybridization system. Furthermore, the TDHG as a sustainable power supply for practical applications is also demonstrated. A total of 912 green light-emitting diodes (LEDs) with a diameter of 5 mm in series can be lit up directly at a low operation frequency of 1 Hz, and several commercial electronics are also sustainably driven, confirming the feasibility of the TDHG as a potential device to be applied for mechanical energy harvesting. This work may provide a new concept for hybrid energy harvester design with superior performance.

2. Results and Discussion

2.1. Device Structure

As the 3D schematic diagram shown in **Figure 1**A, the TDHG is a simple and portable device, which is composed of a circular-shaped DEG and two stacked arc-shaped TENGs. To be specific, the upper part is a DEG that consists of a uniformly pre-stretched annular very high bond (VHB) membrane, clamped on the external perimeter to a fixed acrylic ring frame, and on the inner perimeter to a mobile rigid acrylic disc. A layer of carbon conductive grease is coated on both sides of the elastomer membrane to serve as compliant electrodes. Elastic deformation occurs when an external force is applied on the rigid disc while elastic potential energy is simultaneously stored, and the device will return to its original state when the external force is removed, as exhibited in the top images of Figure 1B. In order to ensure an ideal synchronism action with the DEG component, two stacked arc-shaped TENGs working in vertical contact-separation mode are parallelly connected to each other and arranged under the DEG unit. The design of an arch structure of the TENG (which can be seen more clearly in the lower left image of Figure 1B) contributes to the contact and separation activities between the two friction layers even if under a strong electrostatic adsorption. Polyimide (Kapton) film and spring steel sheet are selected as the tribo-layers due to their different electron affinity according to the triboelectric series,[50] and the spring steel sheet also acts as an electrode while an aluminum (Al) foil adhered under the Kapton film serves as the other electrode. More than that, a holey soft foam is attached to the back side of the steel sheet to ensure a sufficient contact between the two friction layers, aiming at a greater output. One can also note that an acrylic plate is placed between DEG and TENG in order to guarantee a uniform force distribution on the TENG unit under DEG vibration, thus improving the contact status of the friction layers. The detailed fabrication process of the whole device will be explained in the Experimental Section.

2.2. Working Principle

Owing to their essential features, both of TENG and DEG can be thought of as variable capacitor-like generators, and their working mechanisms are depicted in Figures S1 and S2A and Note S1, Supporting Information, respectively. Figure 1C illustrates the simplified circuit scheme (the complete circuit is shown in Figure S3A, Supporting Information) and working principle of TDHG. As can be seen, the DEG and TENG are in a parallel connection and connected to a simplest (1-order) SEC.[35,39,47,51] Initially, all generators and capacitors are discharged (state i). After one stretching-release operation of DEG, contact-separation motion is induced to the TENG, and consequently producing an output voltage. Thanks to the circuit as designed, this voltage not only charges the external capacitors (C_1 and C_2), but also serves as bias voltage for the DEG, and thereby, DEG has obtained the polarization charges and can be continuously operated.

To elaborate the fundamental self-charge excitation mechanism, for simplicity, the TDHG is considered as a simple

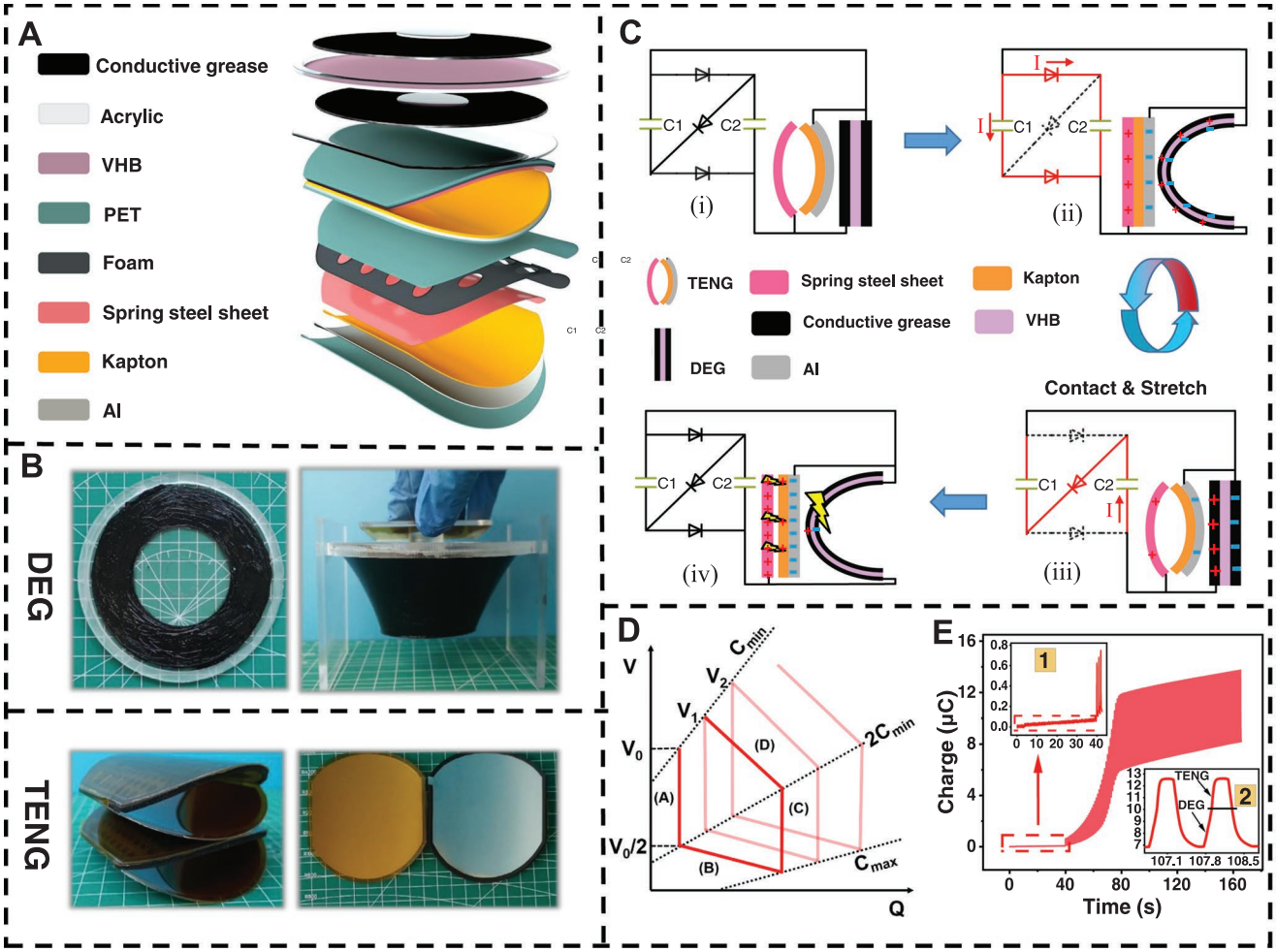

Figure 1. Structural design and working mechanism of TDHG. A) Structural schematic of TDHG. B) Photographs of the as-fabricated DEG and arc-shaped TENG. C) Working principle of the self-excitation TDHG. D) Energy harvesting cycle of TDHG in the *Q*–*V* plane. E) Charge accumulation process of TDHG in absence and presence of TENG. Insets illustrate the enlarged charge curves (1) before and (2) after TENG connected into the circuit, respectively.

variable capacitor with an initial (minimum) capacitance of C_{min} and a maximum capacitance of C_{max}, and the capacitance of C_1 and C_2 is defined as C. We assume TENG charges both the TDHG and SEC up to a voltage V_0 by its first contact-separation, and thus charge on the TDHG at that moment can be described as:

$$Q_0 = C_{min} V_0 \tag{1}$$

The detailed charge excitation process is demonstrated in Figure 1D. When the DEG is stretched again and impacts the TENG to get contact, the capacitance of TDHG increases rapidly, leading to a voltage drop (segment A). Since all three diodes are reverse biased, the charges are trapped on the device until its voltage decreases to $V_0/2$. At this point, the SEC toggles to its parallel configuration (state ii in Figure 1C), and charges transfer from SEC to TDHG to get a potential equilibrium (segment B). When the DEG starts to relax and the TENG gets separated, the TDHG switches to a low capacitance/high voltage form (segment C), and the SEC toggles again to its open-circuit status. Once the voltage of the TDHG doubles, the SEC takes its series configuration (state iii in Figure 1C) and enables charges flowing from TDHG to SEC (segment D). This back and forth charge exchange allows the self-priming circuit to convert the generated energy to a higher charge form, and the cycle will end up at a voltage $V_1 = \alpha V_0$, where α stands for the voltage increase rate and can be expressed as:

$$\alpha = \frac{2(C_{min} + C)(C_{max} + C)}{(C_{max} + 2C)(2C_{min} + C)} \tag{2}$$

The detailed derivation of α is discussed in Note S2, Supporting Information. After K cycles, the voltage on the TDHG will be boosted to $\alpha^K V_0$, which results in an excited charge of:

$$Q_K = \alpha^K V_0 C_{min} \tag{3}$$

However, an excessive charge excitation would lead to dielectric breakdown and air breakdown in DEG and TENG, respectively (state iv in Figure 1C). As a result, the output of TENG

will sharply decrease, and the difference is that the DEG will be destroyed.

Benefiting from this novel hybridization, the energy generated by TENG can be directly used to polarize DEG, so that these two harvesters can work together to obtain a greater output. This solution, compared to other methods such as commercial high-voltage source[51] or DC power supply[38] for DEG operation, presents the advantages to be more feasible, economical, and environmental friendly, which demonstrates great significance for promoting the practical applications of DEG. Furthermore, the application range of TENG has been expanded as well. To further confirm the importance of TENG for DEG polarization, the charge characteristic of the system was monitored both in absence and presence of TENG. As shown in Figure 1E, no charge transfers between DEG and the SEC within the first 40 s (inset 1), but impressively, the charge increases rapidly once the TENG connected in and the two scavengers subsequently start to work together (inset 2).

2.3. Basic Electrical Performances

Since the output performance of TDHG is superimposed by that of the DEG and TENG, the separate investigation of each individual component should be very critical, and a linear motor was utilized to contribute to the stretching-release activity of DEG and contact-separation action of TENG (**Figure 2**A). The dynamic output charge curves under an operation frequency of 0.5 Hz for TENG, DEG and TDHG are depicted in Figure 2B, and their corresponding enlarged images are shown in Figure 2C. As illustrated, for the TENG part, the transferred charges increase with operation time in the initial stage, while the baseline begins to shift up after charge reaches a maximum value of 2.07 μC. The reason for this variation trend is that air breakdown occurs between the two electrodes when the surface charge density exceeds a critical amount. After that, the dielectric film would be positively (oppositely) charged during corona

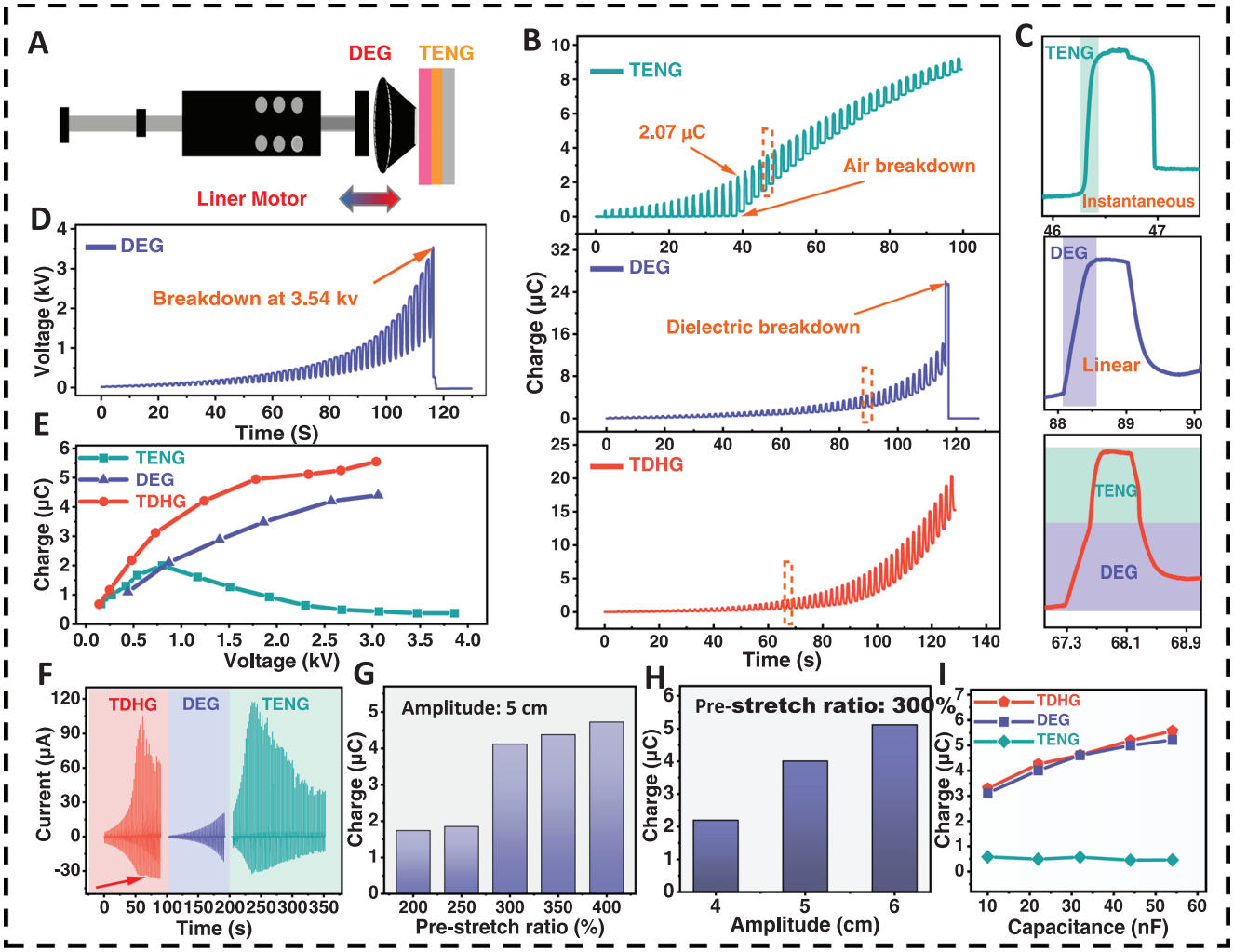

Figure 2. Basic electrical performances of TENG, DEG, and TDHG under an operation frequency of 0.5 Hz. A) Schematic diagram of the operation process. B) Charge accumulation processes of TENG, DEG, and TDHG under continuous operation. C) The detailed output charge curves from the dashed areas of TENG, DEG, and TDHG, respectively. D) Voltage-boost process of DEG at a deformation amplitude of 5 cm. E) The output charge of TENG, DEG, and TDHG at diverse excitation voltages. F) Dynamic current of TDHG, DEG, and TENG. Output charge of DEG under G) different pre-stretch ratios and H) deformation amplitudes when the voltage excited to 2600 V. I) The charge of TENG, DEG, and TDHG when adopting different external capacitance in the SEC.

discharge process as shown in Figure S2B, Supporting Information, thereby locks equivalent charges on the bottom Al electrode and reduces charge quantity that can be transferred. The experimental result signifies that although the output charge can be effectively improved by the SEC, air breakdown is the main restriction that limits the performance of TENG.

In contrast, DEG is free from the limitation of air breakdown owing to its unique configuration that no air gap between the dielectric material and soft electrode. To evaluate the output characteristic of the DEG under continuous excitation (deformation amplitude of 5 cm), a circuit shown in Figure S3B, Supporting Information, was adopted, where TENG was only employed as a polarization source for DEG and was removed after the DEG obtaining an basic voltage of 30 V. The results imply that both of voltage (Figure 2D) and charge produced by DEG exhibit an exponential growth as the operating cycle increasing, which will persist until dielectric breakdown occurs. Since the occurrence of dielectric breakdown is much more difficult than air breakdown due to a more intensive electric field is required (proportional to the dielectric constant of the dielectric film),[42,43] a long-term charge accumulation of DEG compared to TENG is ensured. Herein, for the selected 0.5 mm thick VHB4905 membrane with a pre-stretching ratio of 300%, which can withstand the maximum excitation voltage of 3.54 kV, the maximum output charge is 4.2 μC. It is worth emphasizing that the breakdown strength of DEG can be further improved by optimizing the properties of dielectric materials.

Interestingly, the two energy conversion technologies demonstrate distinct output characteristics, that the charge pulse signal of TENG is transient because the charge transfer takes place at the instant of contact-separation, while the curve of DEG exhibits a gradually increased linear feature since the device takes a certain amount of time to overcome the elastic potential energy during the stretching and releasing process, as depicted in top two images of Figure 2C. After assembling, the TDHG shows a good combination output of the two components, implying that the TENG and DEG can work in a synchronism manner. Moreover, although the charge of TENG will gradually decay after reaching the maximum value, the charge of the DEG increases with the operating cycle growth, which leads the charge feature of TDHG to be dominated by DEG, as illustrated in Figure 2E.

The output current signals of different generators are shown in Figure 2F. Obviously, for a specific energy harvester at a constant working frequency, the current will demonstrate the same trend of its charge according to:

$$I = \frac{dQ}{dt} \tag{4}$$

Therefore, the current of DEG exhibits a symmetrical exponential rise curve, while that of TENG increases first and then decreases due to air breakdown occurrence. Owing to the positive current of TENG is much higher than that of the DEG, the positive part of TDHG current is dominated by TENG, but thanks to the oscillatory rise negative current of DEG, the negative current of TDHG keeps rising after TENG suffering from air breakdown.

2.4. Performance Optimization

In order to get an optimal output, some intrinsic factors that influence the performance of TDHG have been investigated. For the DEG part, various pre-stretching ratio of DE film (namely the final area of the VHB membrane stretched to the ring frame/its original size) and operation amplitude affecting on the output performance have been experimentally tested when the voltage reached to 2600 V with a constant operating frequency of 0.5 Hz. As depicted in Figure 2G,H, a larger pre-stretching ratio and a greater deformation amplitude will result in a relatively greater output. Since the change of capacitance between the stretched and released configurations determines the energy output of DEG (as discussed in Note S1, Supporting Information), the capacitance variation trend of DEG has been systematically studied under various pre-stretch ratios and operating amplitudes. As depicted in Figure S4, Supporting Information, a sharp increase in capacitance variation is observed with the increase of pre-stretch ratio at the same device displacement, which implies that a larger pre-stretch ratio will lead to a greater output performance. Moreover, for a constant pre-stretch ratio, the increase in device displacement leads to a capacitance enlargement and an improved output performance consequently. However, an excessive deformation may lead to DE film rupture due to the elasticity limitation, which is detrimental to stable energy harvesting. Therefore, a pre-stretching ratio of 300% and operation amplitude of 5 cm will be selected to achieve a relatively large but reliable output in the subsequent experiments.

Another parameter that highly influences the performance of TDHG system should be the capacitance of external capacitors in the SEC. In theory, a larger external capacitor would lead to a higher charge transfer,[35,39,47] which is proved by experimental results (Figure 2I). However, a larger external capacitor spends a longer time to reach charge saturation, which is not favorable for practical applications. Therefore, on balance, we adopted 22 nF external capacitance for the separate TENG and DEG characterization in the following tests, but a 44 nF capacitor was selected for TDHG whose capacitance is superimposed by the capacitance of TENG and DEG.

Based on the above discussion, it can be known that though DEG can produce a higher charge output at a greater excitation voltage, the possibility of device damage is the major threat. At the same time, the charge of TENG will decrease when the excitation voltage exceeds the critical value. Therefore, maintaining the excitation voltage of the TDHG at a proper value can not only guarantee a relatively maximum charge output, but also protect the device away from destruction. Therefore, a Zener diode was used to release the surplus charges to achieve an appropriate voltage (**Figure 3**A). As depicted in Figure 3B, by utilizing different Zener diodes, the charge of the TDHG increases with the stabilized voltage (stabilivolt) growth. However, when the excitation voltage exceeds 1600 V, the charge increment of TDHG is not particularly significant. Hence, the excitation voltage will be stabilized at 1600 V for the following tests.

Under the above optimized conditions, the performances of TENG, DEG, and TDHG were characterized at 0.5 Hz, and the results indicate their output charges can reach 1.03, 3.03, and 5.05 μC, respectively, as shown in Figure 3C. Obviously,

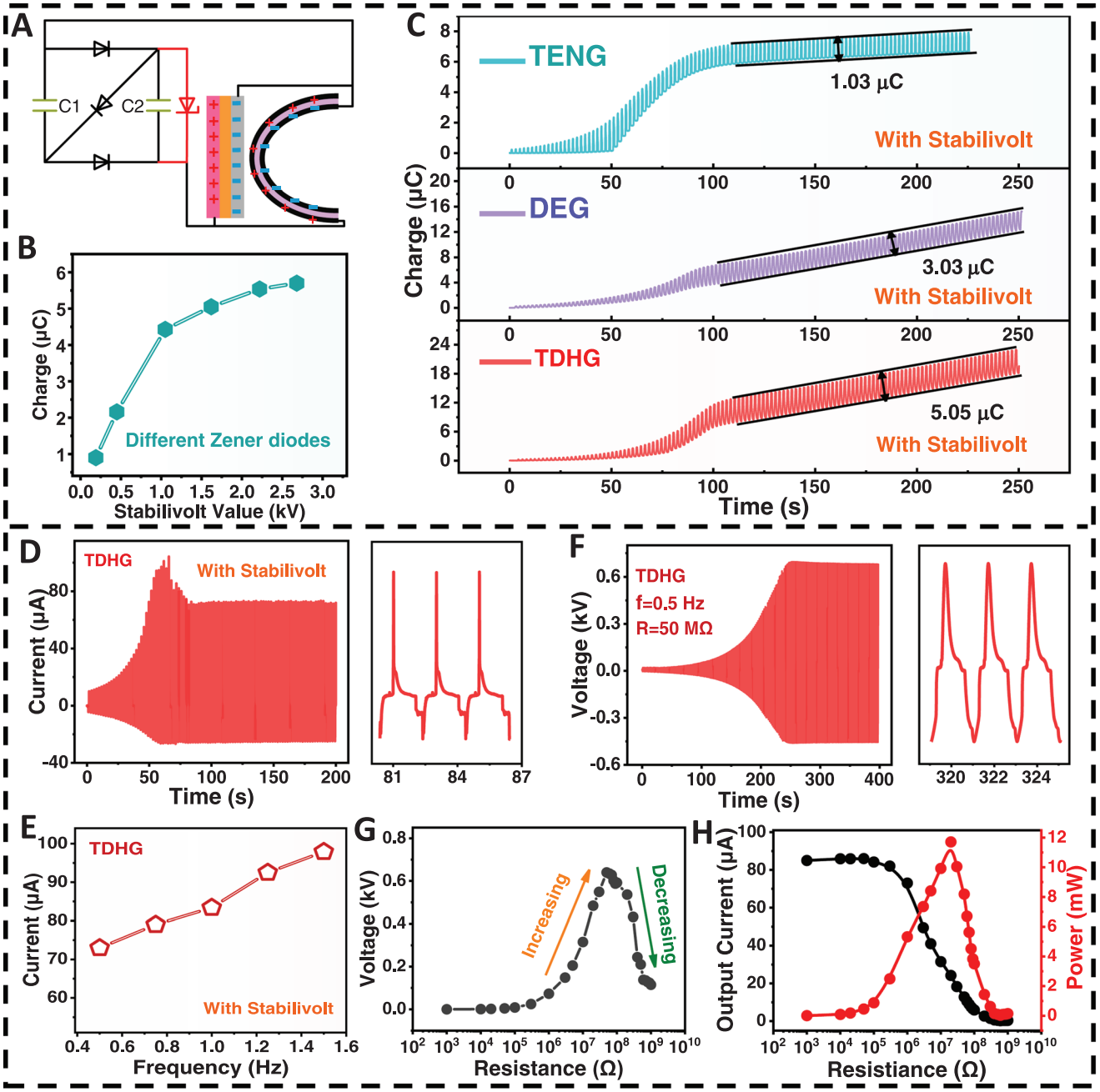

Figure 3. Electrical performances of TENG, DEG, and TDHG with voltage stabilization. A) Schematic diagram of the voltage stabilization circuit. B) Charge of TDHG by adopting different Zener diodes. C) Dynamic charge variation processes of TENG, DEG, and TDHG at a stabilized voltage (stabilivolt) of 1600 V. D) Dynamic current variation of TDHG at the optimal condition with its enlarged curve at the right side. E) The current of TDHG with voltage stabilization (1600 V) under various operation frequencies. F) Dynamic output voltage of TDHG at the optimal condition on an external load of 50 MΩ, and the right side is the enlarged curve. G) The voltage and H) current and power output of TDHG with voltage stabilization (1600 V) under various external loads at 1 Hz.

DEG demonstrates a superior energy generation performance than TENG, and after assembling, the output charge of TDHG performs around fivefold enhancement of individual TENG generated, which affirms the superiority of this novel hybridization. Moreover, the performance of TDHG could be further improved by optimizing dielectric material of DEG and utilizing a SEC with a higher number of stages. In addition, after voltage stabilization, the short-circuit current of TDHG reaches to the stable state in 65 s, then tends to be long-term stable (Figure 3D). Certainly, operation frequency has great impact on the short-circuit current according to Equation (4), and experimental result (Figure 3E) reveals that the stable output current can be tuned from 73 to 97.9 μA by varying the frequency from 0.5 to 1.5 Hz. Apart from short-circuit current, output voltage

on the load should be another main parameter for performance evaluation of a generator. Thus, a load of 50 MΩ was chosen for load voltage measurement and a constant voltage of 698 V was obtained (Figure 3F).

To explore the output capability of TDHG, the output voltages and currents on varied load resistances have been measured under an operation frequency of 1 Hz. As illustrated in Figure 3G,H, with the increment of load resistance, the output voltage raises first and subsequently decreases, which can be ascribed to that excessively large resistance will hinder the charge transfer activity in this SEC and thus reduces the voltage excitation capability. Furthermore, on account of Ohm loss, the output current declines gradually with the external load increasing and the maximum instantaneous power of TDHG can reach 11.7 mW when the load resistance is 20 MΩ. Moreover, the energy conversion efficiency, which should be critically important to a potential power source, can be calculated by the ratio between the generated electrical energy and the input mechanical energy. As depicted in Figure S5, Supporting Information, the total input mechanical energy and electrical energies generated by the three generators during one operation cycle are calculated as 0.00619 J (input mechanical energy), 0.00198 J (TDHG), 0.000817 J (DEG), and 0.000222 J (TENG), respectively. Benefiting from the high peak power contributed by TENG and long output duration guaranteed by DEG, the TDHG achieves an energy conversion efficiency of 32%, which is much higher than that of the sole TENG (3.6%) and DEG (13.2%). This experimental result further confirms the superiority of this novel hybridization system, which not only overcomes the restrictions of DEG and TENG, but also greatly improves the energy conversion efficiency of the system.

Additionally, to determine the long-term stability of the system, the short-circuit current (I_{SC}) of TDHG is tested at a frequency of 1.3 Hz. As shown in Figure S6, Supporting Information, the I_{SC} decreases slightly (90.1–87.6 μA, remains 97.23% of its initial value) after continuous testing of 10 000 cycles at a room temperature, and keeps stable at a wide temperature range (10–50 °), proving ideal stability of the TDHG for practical applications.

The above results prove that the novel-designed TDHG does not only manifest excellent performance to harvest low-frequency ambient mechanical energies, but also has great potential for driving some electronics with higher power consumption to realize a self-powered system.

3. Practical Applications

To demonstrate the potential and feasibility of TDHG as a power supply, the capability of the fabricated device for driving various electronic devices are depicted in **Figure 4**. First, as an energy harvester, the harvesting energy of TDHG can be stored in capacitors for the subsequent utilization. Hence, with the help of a rectification circuit (Figure 4A), the charging capabilities of individual TENG, DEG, and TDHG were investigated at a constant operating frequency of 1 Hz. As illustrated in Figure 4B, for a 470 μF capacitor, in 300 s, the TDHG can charge it to 5.8 V, and DEG can charge it to 3.2 V, whereas TENG can only charge it to 1.4 V. This result undoubtedly verifies the higher energy conversion efficiency of TDHG compared to DEG and TENG, and also highlights the practicability of this novel hybrid generator. Besides, the performance of TDHG was further investigated by charging different capacitors (1, 100, 470 μF, 1 mF) as shown in Figure 4C. As can be seen, in 300 s, the capacitors of 100, 470 μF, and 1 mF can be charged to 24.3, 5.8, and 2.5 V, respectively. Moreover, 4.73 V can be charged into a 1 μF capacitor by every single step operation (around 1 s), which is much more outstanding than the previous reported charge-excitation TENG work[35] (a milestone report in TENG research filed) even under a much lower working frequency (1 Hz herein and 4 Hz in Ref.[35]), further confirming the superiority of hybridization of DEG with TENG. The self-powered systems were built by integrating TDHG with a commercial capacitor (100 μF) as the energy storage part, and a commercial calculator could be powered for carrying out complicated calculations at 1 Hz (as shown in Figure 4D,E, and Movie S1, Supporting Information). More than that, a commercial thermo-hygrometer could be driven for continuous working under a 3 Hz operation (Figure 4F,G and Movie S2, Supporting Information). Finally, as an intuitive demonstration, 912 LEDs in series were linked to the as-fabricated TDHG, all of which could be lit to high brightness by a linear motor (operation frequency of 1 Hz, Figure 4H,I and Movie S3, Supporting Information) or a simple footstep (Movie S4, Supporting Information), further indicating the potential of the TDHG as a sustainable power source.

4. Conclusions

In this work, a hybrid generator composed of TENG and DEG has been proposed for the first time to effectively harvest the widely distributed ambient mechanical energy. Unlike conventional charge-excitation TENG work, herein we adopt DEG working with TENG in a SEC. This innovative design demonstrates several superior performances. First, owing to their similarity in electricity generation mechanism and transmission, the two scavengers can work cooperatively with each other. Second, benefitting from this novel design, the intrinsic limitations of these two energy harvesting technologies including low energy output capability of TENG caused by air-breakdown effect and external polarization voltage requirement for DEG have been effectively resolved. After hybridization, the voltage generated by TENG can act as polarization source for DEG, while the no air-gap configuration of DEG can guarantee an exceptional energy output of the hybrid system. At the optimized condition, the as-fabricated TDHG can deliver an output charge of 5.05 μC, which is about fivefold enhancement in comparison to that of the normal charge-excitation TENG, and the performance is hopeful to be further improved by optimizing dielectric material of DEG and utilizing a higher-ordered SEC. Furthermore, the system energy conversion efficiency has been significantly improved due to the mutual beneficial interaction between TENG and DEG. This work provides a new concept of self-excitation hybrid generator to achieve high and stable power generation, which not only significantly facilitates the practical applications of TENGs and DEGs, but also promotes the development of large scale self-powered systems based on ambient mechanical energy harvesting.

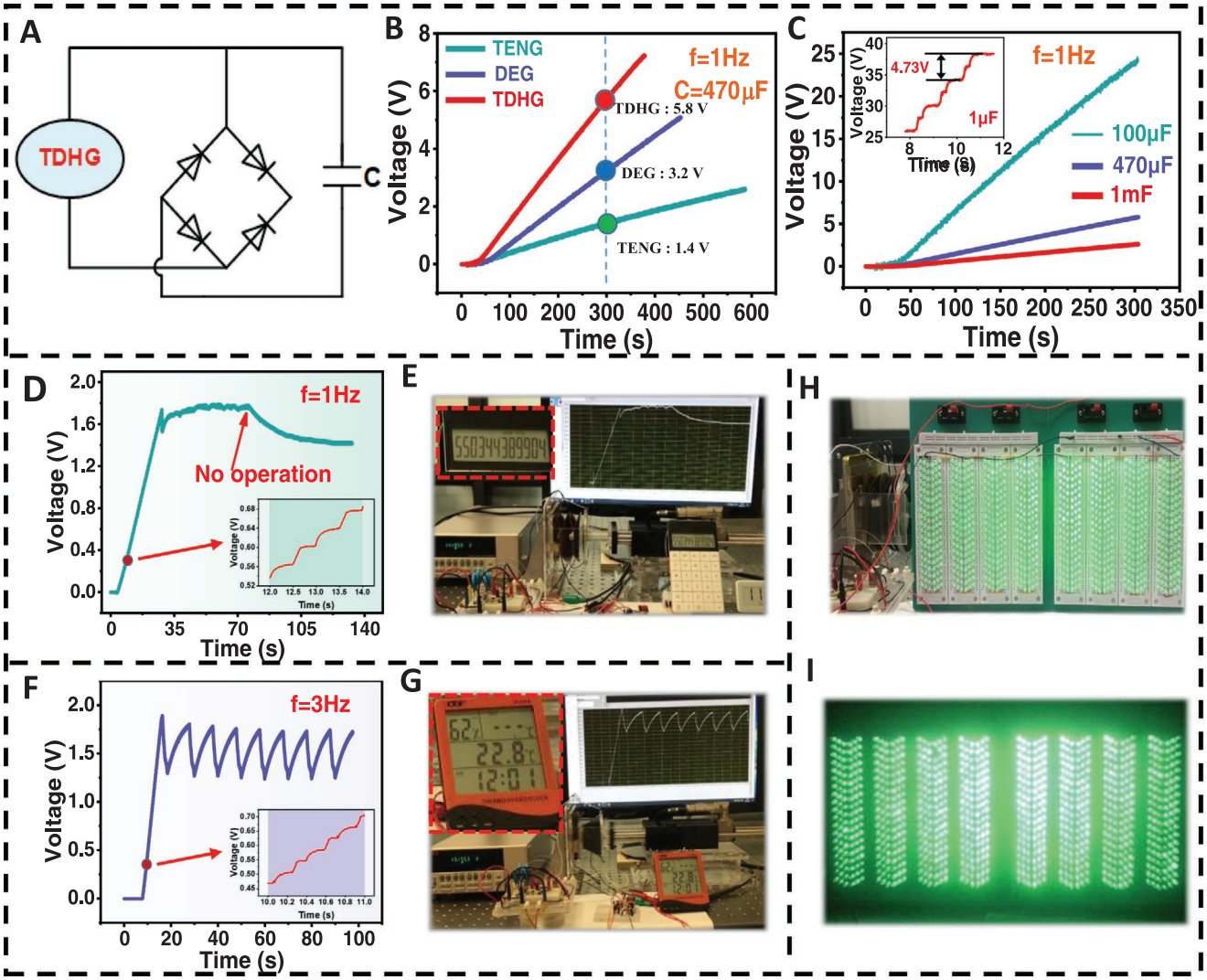

Figure 4. Practical applications of TDHG. A) Circuit diagram for charging capacitors. B) Voltage profile of 470 μF capacitor charged by single TENG, DEG, and TDHG at 1 Hz. C) Charging curves of 100, 470 μF, 1 mF, and 1 μF (inset) commercial capacitors charged by TDHG at 1 Hz. D–G) Voltage curves of the storage capacitor and photographs for the TDHG powering D,E) a commercial calculator (frequency: 1 Hz) and F,G) thermo-hygrometer (frequency: 3 Hz). H,I) Directly powering 912 green LEDs by TDHG under 1 Hz both in bright and dark environment.

5. Experimental Section

Fabrication of the Dielectric Elastomer Generator: First, a thin sheet of acrylic elastomer membrane (VHB 4905, 3M) with an original thickness of 0.5 mm was selected as the dielectric layer, and its permittivity and loss factor were 4.05 and 0 at low operation frequencies, respectively. Then, two acrylic annuli (4 mm in thickness) with an inner diameter of 10 cm were fabricated by laser cutting technique and served as the frame to stretch and clamp VHB film, and thus, the pre-stretch ratio of VHB film could be adjusted by altering the initial radii of the membrane to match the experimental requirements. After fixing the VHB film on the acrylic annulus, two rigid acrylic discs (2 mm in thickness and 5.4 cm in diameter) were adhered to the center of the membrane from both sides for coupling the DEG to mechanical loads and ensuring a uniform strain distribution. Finally, the compliant electrodes were made by brushing conductive grease (GV-80S) onto the remaining area of the VHB membrane.

Fabrication of the Triboelectric Nanogenerator: As shown in Figure 1B, the TENG part was made up of two stacked identical units. For each unit, the fabrication process was as follows: First, two arc-shaped polyethylene terephthalate (PET) sheets with a thickness of 0.5 mm were cut into a circular shape (10 cm in diameter) by laser cutting technique and selected as the substrate material, and then, both of the bilateral sides were carved 6 mm away to shape straight edges for facilitating the subsequent device assembling. To guarantee a sufficient contact between the tribo-layers, a holey soft foam (2 mm in thickness, and the diameter of each hole was 4 mm) was cut into the same shape, and adhered on the inner side of the PET substrate. After that, a spring steel sheet (0.06 mm in thickness, corresponding stiffness was 27.2 N m^{-1}) was attached to the foam surface acting as the contact electrode. For the other side of TENG, Kapton film (50 μm in thickness), Al foil (20 μm in thickness), and PET sheet were sequentially attached to each other layer-by-layer. Then, the two as-fabricated composite films were mounted face-to-face with each other along the straight edges by Kapton tape. One could also note that, although the spring steel sheet and Al foil held the same configurations of the PET substrate, their diameters were 6 mm smaller to avoid the short-circuit contact between the two electrodes. After assembling, the two arc-shaped TENGs (corresponding stiffness was 134.1 N m^{-1}) and as-fabricated DEG (corresponding stiffness was 254.9 N m^{-1}) were stacked one next to the other by bonding their center points with a double-side Kapton tape, and finally, the hybrid TDHG was obtained (corresponding stiffness was 333.16 N m^{-1}).

Measurement: The contact-separation process of TENG and deformation of DEG were carried out by a line motor (WEINERMOTOR WMU-090-D) with sinusoidal motion. The voltage signals of the generators were measured by an electrostatic voltmeter (Trek 370), and the transferred charges and short-circuit currents were measured by an electrometer (Keithley 6514).

Supporting Information

Supporting Information is available from the Wiley Online Library or from the author.

Acknowledgements

The authors gratefully acknowledge the financial support from the National Key Research and Development Project (Grant No. 2021YFA1201600), National Natural Science Foundation of China (Grant No. 52076024), Natural Science Foundation of Chongqing (Grant No. cstc2021jcyj-msxmX0625), and the Fundamental Research Funds for the Central Universities (Grant Nos. 2019CDXZWL001 and 2020CDCGJ005).

Conflict of Interest

The authors declare no conflict of interest.

Author Contributions

J.W., W.L., and Q.Z. contributed equally to this work. X.W. supervised the project. Z.L.W., X.W., J.W., and Q.Z. conceived the idea, analyzed the data, and wrote the paper. W.L. proposed the coupling design to obtain the positive output superposition of DEG and TENG by using the self-charge-excitation principle. J.W., Q.Z., Y.Z., and H.G. designed and optimized the structure of TDHG. W.H., X.Z., and Y.L. helped with the experiments. All the authors discussed the results and commented on the manuscript.

Data Availability Statement

The data that support the findings of this study are available from the corresponding author upon reasonable request.

Keywords

dielectric elastomer generators, mutual boosting, self-excitation, triboelectric nanogenerators

Received: September 15, 2022
Revised: October 13, 2022
Published online:

[1] Z. L. Wang, *Mater. Today* **2017**, *20*, 74.
[2] C. Wu, A. C. Wang, W. Ding, H. Guo, Z. L. Wang, *Adv. Energy Mater.* **2019**, *9*, 1802906.
[3] W. G. Kim, D. W. Kim, I. W. Tcho, J. K. Kim, M. S. Kim, Y. K. Choi, *ACS Nano* **2021**, *15*, 258.
[4] X. Zhao, H. Askari, J. Chen, *Joule* **2021**, *5*, 1391.
[5] Q. Shi, Z. Sun, Z. Zhang, C. Lee, *Research* **2021**, *2021*, 6849171.
[6] F.-R. Fan, Z.-Q. Tian, Z. L. Wang, *Nano Energy* **2012**, *1*, 328.
[7] Z. L. Wang, A. C. Wang, *Mater. Today* **2019**, *30*, 34.
[8] Y. Bai, H. Jantunen, J. Juuti, *Adv. Mater.* **2018**, *30*, 1707271.
[9] A. M. El-Mohandes, R. Zheng, *Nano Energy* **2021**, *80*, 105588.
[10] J. Kim, H. Cho, M. Han, Y. Jung, S. S. Kwak, H. J. Yoon, B. Park, H. Kim, H. Kim, J. Park, S. W. Kim, *Adv. Energy Mater.* **2020**, *10*, 2002312.
[11] C. Zhang, L. He, L. Zhou, O. Yang, W. Yuan, X. Wei, Y. Liu, L. Lu, J. Wang, Z. L. Wang, *Joule* **2021**, *5*, 1613.
[12] R. Hinchet, H.-J. Yoon, H. Ryu, M.-K. Kim, E.-K. Chol, D.-S. Kim, S.-W. Kim, *Science* **2019**, *365*, 491.
[13] W. Xu, H. Zheng, Y. Liu, X. Zhou, C. Zhang, Y. Song, X. Deng, M. Leung, Z. Yang, R. X. Xu, Z. L. Wang, X. C. Zeng, Z. Wang, *Nature* **2020**, *578*, 392.
[14] M. Wang, J. Pan, M. Wang, T. Sun, J. Ju, Y. Tang, J. Wang, W. Mao, Y. Wang, J. Zhu, *ACS Sustainable Chem. Eng.* **2020**, *8*, 3865.
[15] Y. X. Shi, F. Wang, J. W. Tian, S. Y. Li, E. G. Fu, J. H. Nie, R. Lei, Y. F. Ding, X. Y. Chen, Z. L. Wang, *Sci. Adv.* **2021**, *7*, eabe2943.
[16] H. E. Lee, J. H. Park, D. Jang, J. H. Shin, T. H. Im, J. H. Lee, S. K. Hong, H. S. Wang, M. S. Kwak, M. Peddigari, C. K. Jeong, Y. Min, C. H. Park, J.-J. Choi, J. Ryu, W.-H. Yoon, D. Kim, K. J. Lee, G.-T. Hwang, *Nano Energy* **2020**, *75*, 104951.
[17] C. Rodrigues, D. Nunes, D. Clemente, N. Mathias, J. M. Correia, P. Rosa-Santos, F. Taveira-Pinto, T. Morais, A. M. Pereira, J. Ventura, *Energy Environ. Sci.* **2020**, *13*, 2657.
[18] X. J. Pu, H. Y. Guo, J. Chen, X. Wang, Y. Xi, C. G. Hu, Z. L. Wang, *Sci. Adv.* **2017**, *3*, e1700694.
[19] M. Zhu, Z. Sun, T. Chen, C. Lee, *Nat. Commun.* **2021**, *12*, 2692.
[20] M. Zhu, Z. Yi, B. Yang, C. Lee, *Nano Today* **2021**, *36*, 101016.
[21] J. Sun, L. Zhang, Z. Li, Q. Tang, J. Chen, Y. Huang, C. Hu, H. Guo, Y. Peng, Z. L. Wang, *Adv. Mater.* **2021**, *33*, 2102765.
[22] R. Lei, Y. Shi, Y. Ding, J. Nie, S. Li, F. Wang, H. Zhai, X. Chen, Z. L. Wang, *Energy Environ. Sci.* **2020**, *13*, 2178.
[23] H. Guo, J. Chen, L. Wang, A. C. Wang, Y. Li, C. An, J.-H. He, C. Hu, V. K. S. Hsiao, Z. L. Wang, *Nat. Sustain.* **2020**, *4*, 147.
[24] Y. Zi, S. Niu, J. Wang, Z. Wen, W. Tang, Z. L. Wang, *Nat. Commun.* **2015**, *6*, 8376.
[25] Z. L. Wang, J. Chen, L. Lin, *Energy Environ. Sci.* **2015**, *8*, 2250.
[26] H. Askari, E. Asadi, Z. Saadatnia, A. Khajepour, M. B. Khamesee, J. Zu, *Nano Energy* **2017**, *32*, 105.
[27] H. Askari, Z. Saadatnia, E. Asadi, A. Khajepour, M. B. Khamesee, J. Zu, *Nano Energy* **2018**, *45*, 319.
[28] R. Fallahpour, R. Melnik, *Measurement* **2021**, *175*, 109136.
[29] L. Wang, Y. Wang, H. Wang, G. Xu, A. Doring, W. A. Daoud, J. Xu, A. L. Rogach, Y. Xi, Y. Zi, *ACS Nano* **2020**, *14*, 10359.
[30] Z. Q. Liu, Y. Z. Huang, Y. X. Shi, X. L. Tao, H. Z. He, F. D. Chen, Z. X. Huang, Z. L. Wang, X. Y. Chen, J. P. Qu, *Nat. Commun.* **2022**, *13*, 4083.
[31] S. Y. Li, J. Nie, Y. X. Shi, X. L. Tao, F. Wang, J. W. Tian, S. Q. Lin, X. Y. Chen, Z. L. Wang, *Adv. Mater.* **2020**, *32*, 2001307.
[32] S. Wang, Y. Xie, S. Niu, L. Lin, C. Liu, Y. S. Zhou, Z. L. Wang, *Adv. Mater.* **2014**, *26*, 6720.
[33] L. Cheng, Q. Xu, Y. Zheng, X. Jia, Y. Qin, *Nat. Commun.* **2018**, *9*, 3773.
[34] L. Xu, T. Z. Bu, X. D. Yang, C. Zhang, Z. L. Wang, *Nano Energy* **2018**, *49*, 625.
[35] W. Liu, Z. Wang, G. Wang, G. Liu, J. Chen, X. Pu, Y. Xi, X. Wang, H. Guo, C. Hu, Z. L. Wang, *Nat. Commun.* **2019**, *10*, 1426.
[36] J. Wang, C. Wu, Y. Dai, Z. Zhao, A. Wang, T. Zhang, Z. L. Wang, *Nat. Commun.* **2017**, *8*, 88.
[37] J. Fu, G. Xu, C. Li, X. Xia, D. Guan, J. Li, Z. Huang, Y. Zi, *Adv. Sci.* **2020**, *7*, 2001757.
[38] Y. Jiang, S. Liu, M. Zhong, L. Zhang, N. Ning, M. Tian, *Nano Energy* **2020**, *71*, 104606.

[39] G. Moretti, S. Rosset, R. Vertechy, I. Anderson, M. Fontana, *Adv Intell Syst* **2020**, *2*, 2000125.
[40] H. Liu, J. Zhong, C. Lee, S.-W. Lee, L. Lin, *Appl. Phys. Rev.* **2018**, *5*, 041306.
[41] S. Chiba, M. Waki, *Sustainable Chem. Pharm.* **2020**, *15*, 100205.
[42] Y. Zi, C. Wu, W. Ding, Z. L. Wang, *Adv. Funct. Mater.* **2017**, *27*, 1700049.
[43] C. Jiang, K. Dai, F. Yi, Y. Han, X. Wang, Z. You, *Nano Energy* **2018**, *53*, 706.
[44] S. Shian, J. Huang, S. Zhu, D. R. Clarke, *Adv. Mater.* **2014**, *26*, 6617.
[45] J. Huang, S. Shian, Z. Suo, D. R. Clarke, *Adv. Funct. Mater.* **2013**, *23*, 5056.
[46] C. Lagomarsini, C. Jean-Mistral, G. Lombardi, A. Sylvestre, *Smart Mater. Struct.* **2019**, *28*, 035003.
[47] T. McKay, B. O'Brien, E. Calius, I. Anderson, *Smart Mater. Struct.* **2010**, *19*, 055025.
[48] A. Cornogolub, P.-J. Cottinet, L. Petit, *Smart Mater. Struct.* **2016**, *25*, 095048.
[49] T. Vu-Cong, C. Jean-Mistral, A. Sylvestre, *Smart Mater. Struct.* **2013**, *22*, 025012.
[50] H. Zou, Y. Zhang, L. Guo, P. Wang, X. He, G. Dai, H. Zheng, C. Chen, A. C. Wang, C. Xu, Z. L. Wang, *Nat. Commun.* **2019**, *10*, 1427.
[51] P. Illenberger, K. Takagi, H. Kojima, U. K. Madawala, I. A. Anderson, *IEEE Trans Power Electron* **2017**, *32*, 6904.